Atmos. Chem. Phys. Discuss., 12, 23195–23217, 2012
www.atmos-chem-phys-discuss.net/12/23195/2012/
doi:10.5194/acpd-12-23195-2012
© Author(s) 2012. CC Attribution 3.0 License.

Atmospheric Chemistry and Physics Discussions

This discussion paper is/has been under review for the journal Atmospheric Chemistry and Physics (ACP). Please refer to the corresponding final paper in ACP if available.

A joint effort to deliver satellite retrieved atmospheric CO_2 concentrations for surface flux inversions: the ensemble median algorithm EMMA

M. Reuter[1], H. Bösch[2], H. Bovensmann[1], A. Bril[3], M. Buchwitz[1], A. Butz[4], J. P. Burrows[1], C. W. O'Dell[5], S. Guerlet[6], O. Hasekamp[6], J. Heymann[1], N. Kikuchi[3], S. Oshchepkov[3], R. Parker[2], S. Pfeifer[7], O. Schneising[1], T. Yokota[3], and Y. Yoshida[3]

[1]Institute of Environmental Physics, University of Bremen, Germany
[2]University of Leicester, Department of Physics and Astronomy, Leicester, UK
[3]National Institute for Environmental Studies, Tsukuba, Japan
[4]IMK-ASF, Karlsruhe Institute of Technology, Karlsruhe, Germany
[5]Colorado State University, Fort Collins, CO, USA
[6]Netherlands Institute for Space Research, Utrecht, The Netherlands
[7]Climate Service Center, Helmholtz Zentrum Geesthacht, Hamburg, Germany

Received: 27 July 2012 – Accepted: 29 August 2012 – Published: 7 September 2012

Correspondence to: M. Reuter (maximilian.reuter@iup.physik.uni-bremen.de)

Published by Copernicus Publications on behalf of the European Geosciences Union.

ACPD

12, 23195–23217, 2012

Abstract

We analyze an ensemble of seven XCO_2 retrieval algorithms for SCIAMACHY and GOSAT. The ensemble spread can be interpreted as regional uncertainty and can help to identify locations for new TCCON validation sites. Additionally, we introduce the ensemble median algorithm EMMA combining individual soundings of the seven algorithms into one new dataset. The ensemble takes advantage of the algorithms' independent developments. We find ensemble spreads being often < 1 ppm but rising up to 2 ppm especially in the tropics and East Asia. On the basis of gridded monthly averages, we compare EMMA and all individual algorithms with TCCON and CarbonTracker model results (potential outliers, north/south gradient, seasonal (peak-to-peak) amplitude, standard deviation of the difference). Our findings show that EMMA is a promising candidate for inverse modeling studies. Compared to CarbonTracker, the satellite retrievals find consistently larger north/south gradients (by 0.3 ppm–0.9 ppm) and seasonal amplitudes (by 1.5 ppm–2.0 ppm).

1 Introduction

Our current knowledge about sources and sinks of atmospheric CO_2 is limited by the sparseness of highly accurate and precise CO_2 measurements (Stephens et al., 2007). Due to their global coverage and sensitivity down to the surface, satellite based XCO_2 (the column-average dry-air mole fraction of atmospheric CO_2) retrievals in the near infrared are a promising candidate to reduce existing uncertainties if accurate and precise enough (Rayner and O'Brien, 2001; Houweling et al., 2004; Miller et al., 2007; Chevallier et al., 2007).

At present, seven different retrieval algorithms exist world wide which are under active development in order to meet the demanding user requirements, making them useful for surface flux inversions. These are ACOS v2.9 (O'Dell et al., 2012; Crisp et al., 2012), BESD v01.00.01 (Reuter et al., 2010, 2011), NIES v02.xx (Yoshida et al., 2011),

ACPD
12, 23195–23217, 2012

NIES PPDF-D (Oshchepkov et al., 2008, 2011, 2012), RemoteC v1.0 (Butz et al., 2009, 2011), UOL-FP v3.0 (Bösch et al., 2006, 2011), and WFMD v2.2bcv7b (Schneising et al., 2011, 2012; Heymann et al., 2012). The algorithms are optimized for different instruments (SCIAMACHY, GOSAT), are based on different absorption bands, use different inversion methods (optimal estimation, Tikhonov-Phillips, least squares), based on different physical assumptions (full physics, photon path length probability density function (PPDF), light path proxy), and use different pre- and post-processing filters (e.g. cloud detection from O_2-A band or from a cloud and aerosol imager). Table 1 gives a brief overview of the main conceptual differences of the seven retrieval algorithms. Discussions of the specific strengths and weaknesses and many more points where the individual algorithms differ can be found in the cited literature.

All retrieval teams find encouraging validation results when comparing with TCCON (Total Carbon Column Observing Network) (Washenfelder et al., 2006; Wunch et al., 2011) ground based FTS (Fourier transform spectrometer) measurements (see references above). This goes along with a good inter-algorithm agreement at TCCON sites and with the results of our unified validation study having station-to-station biases typically below 1 ppm and single measurement precisions typically between 2 ppm and 4 ppm (Fig. 1, Table 2).

However, the inter-algorithm agreement as well as the agreement with NOAA's (National Oceanic and Atmospheric Administration) CarbonTracker (Peters et al., 2007, 2010) model (CT2011), i.e. our current knowledge about atmospheric CO_2 based on NOAA's air sampling network, often reduces remote from validations sites due to differing large scale bias patterns (Fig. 2). The user requirements for such bias patterns are demanding; as an example, Miller et al. (2007) and Chevallier et al. (2007) found that regional biases of a few tenths of a ppm can already hamper surface flux inversions.

This indicates that assessing an algorithm's quality should not be based on comparisons against current TCCON stations only. Obviously, large regions of the world possess more "complicated" retrieval conditions without the availability of ground truth measurements which could be used to judge the algorithms' performance.

ACPD
12, 23195–23217, 2012

Diverging model results are common to many scientific disciplines (e.g. Araujo and New, 2007; Rötter et al., 2011), much attention and effort is devoted to this topic on the subject of weather and climate modeling. Here, the divergence of the model results arises not only from structural differences of the different models, but also from the nonlinearity of the model equations, leading to differing results of one single model when performing multiple realizations with slightly differing initial conditions (Hagedorn et al., 2005; Tebaldi and Knutti, 2007). Especially in the case of weather forecasting or climate projections, where no ground truth is available for the verification of the forecasts and projections, it is impossible to identify the "best" model and the "perfect" initial conditions. For long term climate projections, this problem is impaired by the additional unknown future greenhouse forcing. This conceptual problem is dealt with by using multi-model multi-realization multi-emission-scenario ensembles of simulations, which ideally span the entire range of possible model outcomes and thus can be used to estimate the uncertainties of the forecast or projection.

However, interpreting the ensemble's spread as uncertainty is not the only possible application: some studies indicate that the ensemble mean, weighted mean, or median can outperform each individual model under appropriate conditions (e.g. Kharin and Zwiers, 2002; Vautard et al., 2009). Within Sect. 3, we seize this idea and introduce the EnseMble Median Algorithm EMMA with which a global one year data set (June 2009–May 2010) of individual soundings has been generated. It comprises of data from the seven retrieval algorithms mentioned above.

2 Ensemble spread

Due to entirely different samplings (different satellites, different filtering strategies, etc.), any algorithm inter-comparison considering the majority of individual sounding (level 2) can only be based on aggregated data (level 3), in our case monthly averages $10^{\circ} \times 10^{\circ}$. Before gridding, we apply the individual averaging kernels to adjust all retrieval results to a common a priori namely the simple empirical CO_2 model (SECM) of Reuter et al.

ACPD
12, 23195–23217, 2012

(2012). We do this as proposed in the text book of Rodgers (2000) and applied to XCO_2 by, e.g. Reuter et al. (2011). These adjustments are mostly minor, typically a few tenths of a ppm. For consistency, we also remove the overall global bias of each retrieval with SECM as reference.

In order to get statistically robust results, we only use those grid boxes for which the standard error of the mean is estimated to be less than 1 ppm. This takes the individual retrieval precisions into account so that the minimum number of soundings needed to build the average of a grid box can vary from retrieval to retrieval and grid box to grid box. Beforehand, the reported retrieval precision is scaled to match (on average) the precision given in Table 2. TCCON and CT2011 are gridded in the same way.

Figure 2 shows for a typical month (September 2009) the calculated monthly averages. First of all, one can see many large scale similarities such as the north/south gradient. However, one can also find more or less obvious outliers of a few ppm in each of the seven algorithms (e.g. ACOS: Angola, BESD: Amazon, NIES PPDF-D: Saudi Arabia, NIES v02.xx: Senegal, RemoteC: North/East Siberia, UOL-FP: Brazil, WFMD: Somalia).

Often the observed systematic deviations (of level 3 data) are larger than the single sounding retrieval precisions expected from instrumental noise, i.e. they are dominated by specific algorithm effects. Sampling and representation errors are expected to be much lower than the observed deviations and therefore not discussed in this context.

Due to independent algorithm developments, different physical approaches and assumptions, different pre- and post-processing filters, and due to the different instruments, we expect relatively independent bias patterns. This is supported by Fig. 2 showing (uncorrelated) obvious outliers in various regions, i.e. it seems unlikely that all algorithms produce the same bias within one grid box.

This implies that similar averages within one grid box can give us more confidence in the individual retrievals within this grid box. The other way round, large inter-algorithm spreads indicate regions with more difficult and uncertain retrieval conditions.

ACPD
12, 23195–23217, 2012

Therefore, we interpret the ensemble spread, i.e. the standard deviation of (at least five) algorithms, as uncertainty due to regional retrieval biases.

An example is given in Fig. 2 (right, bottom) showing larger inter-algorithm spreads in the tropics and in East Asia (always remote from TCCON sites). This pattern is temporally more or less stable, i.e. similar also in other months.

3 Ensemble median

As described in the previous section, up to seven XCO_2 averages (one for each algorithm) are calculated within each grid box. However, now we are aiming to use the ensemble not only to assess regional and temporal uncertainties but also to create a dataset which is less influenced by regional or temporal biases. This could be achieved, e.g. by building the average, a weighted average, or the median in each grid box.

In this context, the median has some clear advantages: outliers are assumed to be seldom and there is a high chance that a grid box includes no or only one outlying algorithm. Therefore, cancellation of errors cannot be expected. The median is much less sensitive to such individual outliers. Additionally, the median calculates no new quantity from the individuals of an ensemble, it is rather a procedure to select one specific ensemble member. This allows us to easily trace back from level 3 averages to individual level 2 soundings.

Essentially, there are five possible scenarios for median calculation within one grid box: (i) all algorithms perform well and scatter slightly around the true XCO_2 value. In this case the median will help to reduce scatter. (ii) The minority of algorithms produce outliers which influences the median only marginally. (iii) The majority of algorithms produce outliers in different directions. Here it is still likely that the median falls on a well performing algorithm in the "middle". (iv) The majority of algorithms produce outliers in the same direction. This is the only case where the median is a bad choice, because it would select an outlying and ignore a well performing algorithm. As discussed in the

ACPD
12, 23195–23217, 2012

previous section, we assume that the algorithms within one grid box are often realistic with uncorrelated occasional outliers which makes this case very unlikely to happen often. (v) If all algorithms are outlying, the median is not better or worse than selecting any other ensemble member.

We calculate the median only for grid boxes with at least five successfully determined average XCO_2 values. In case of an even number of values, we define the median as that value being closer to the mean. We then trace back to the individual level 2 data which were used to calculate that average being the median. Together with all information needed for inverse modeling (geo-location, time, averaging kernels, etc.), these soundings are stored in the EMMA database.

In order to prevent over-weighting individual algorithms providing considerably larger amounts of data, we limit the maximum number of data points (per grid box) by analyzing the standard error of the mean of each successfully determined average. If the standard error of the mean of the selected algorithm is lower than the 25 % percentile of all algorithms, a centered truncated mean is calculated instead. The (symmetrical) truncation of elements adjusts the standard error of the mean to be slightly larger than the 25 % percentile. In this way, the number of data points can still be rather different but the potential constraint on an inverse model becomes similar.

Summarizing, the EMMA database consists of individual level 2 soundings retrieved by algorithms which can change from grid box to grid box and month to month. Figure 3 shows the integrated data content of each algorithm (defined as $\sum 1/\sigma_i^2$) within the EMMA database. ACOS has the largest integrated data content because it is often selected as median, has many data points per grid box, and a low scatter.

4 Performance of EMMA

The validation of EMMA's level 2 database with TCCON (Fig. 1, Table 2) has been performed analogous to the work of Reuter et al. (2011) and shows very good overall performance: EMMA has more co-locations than any GOSAT retrieval, and a low

ACPD
12, 23195–23217, 2012

station-to-station bias of 0.8 ppm. Mainly due to its WFMD component, EMMA has a single measurement precision of 3.1 ppm which is somewhat larger than most of the GOSAT algorithms. It shall be noted that TCCON's accuracy (2σ) is about 0.8 ppm (Wunch et al., 2010, 2011). This is similar to the observed station-to-station biases of the satellite retrievals and much larger than their differences. Additionally, it shall be noted that the number of co-locations is not solely driven by the satellite retrievals. Due to clouds and instrument maintenance, the seven used TCCON sites provided suitable validation data in less than 40 % of the days.

The following algorithm inter-comparison addresses temporal and spatial bias patterns and is based on gridded level 3 datasets (described in Sect. 2). A glance at Fig. 2 shows that EMMA generates a relatively smooth global map with realistic patterns and no obvious outliers. As mentioned before, we use at least five algorithms to calculate a median. This can result in a loss of coverage relative to some of the individual algorithms.

We calculated the fraction of potential outliers according to unrealistically large spatial gradients ($> 3\,\mathrm{ppm}/10^{\circ}$, Fig. 4, top, left) and unrealistically large deviations from CT2011 (> 3 ppm, Fig. 4, top, middle). EMMA's fraction of potential outliers is below 2 %, which is considerably lower than for any other algorithm. Analyzing the difference between the individual algorithms and EMMA, Fig. 4 shows that large deviations from EMMA are often correlated with large deviations from CT2011 and large gradients.

With respect to the standard deviation of the difference (STDD), EMMA is in better agreement with CT2011 and TCCON than any other algorithm.

We also compared the north/south (N/S) gradient of each month with CT2011 and TCCON by averaging all northern and southern hemispheric grid boxes (using the same sampling). All algorithms agree that CT2011 has a N/S gradient being about 0.3 ppm–0.9 ppm too low. This effect is estimated to be 0.2 ppm less pronounced in the previous CarbonTracker version CT2010. However, it shall be noted that CT2010 ends in 2009 and CO_2 fields after 2009 were estimated by extrapolation from previous years. EMMA's N/S gradients have the third smallest systematic deviations from CT2011 and

ACPD
12, 23195–23217, 2012

the lowest scatter. It has the smallest systematic deviation from TCCON with the third smallest scatter. However, the statistics in comparing to TCCON are less robust because only seven grid boxes include TCCON stations and there are only 12 months for which the N/S gradient has been calculated.

Additionally, we compared the seasonal (peak-to-peak) amplitude of each grid box with CT2011 and TCCON by calculating the difference between annual maximum and minimum. Beforehand, we subtracted a globally constant linear increase of 1.8 ppm yr^{-1}. We considered only those grid boxes with at least six valid months and used the same sampling. Most algorithms agree that CT2011 underestimates the seasonal amplitude by about 1.5 ppm–2.0 ppm, which is broadly consistent with the findings of Yang et al. (2007), Schneising et al. (2011), Reuter et al. (2011), Keppel-Aleks et al. (2012), and Messerschmidt et al. (2012). The effect is estimated to be about 0.3 ppm less pronounced in CT2010 (extrapolated). However some algorithms (especially WFMD) see probably unrealistically large amplitudes. EMMA is in best agreement with CT2011 and in second best agreement with TCCON. It shall be noted that the CT2011 comparison is dominated by the Northern Hemisphere, due to significantly more filled grid boxes. The TCCON statistics are probably not very robust because they rely on seven grid boxes with seasonal cycles only.

5 Conclusions

In a joint effort of all XCO_2 retrieval teams world wide which are actively developing satellite based algorithms for the near infrared, the ensemble median algorithm EMMA has been set up. It takes advantage of the variety of different retrieval algorithms and their independent developments. This allows the reduction of occasional outliers and sometimes unrealistic bias patterns which can be found in each individual retrieval algorithm and which can hamper surface flux inversions.

The EMMA database (June 2009–May 2010) consists of individual XCO_2 retrievals including all information needed for inverse modeling (geo-location, time, averaging

ACPD
12, 23195–23217, 2012

kernels, etc.). It also includes the inter-algorithm spread which gives important information about regional uncertainties.

Analyzing the inter-algorithm spread, we found that the algorithms agree often within < 1 ppm. However, especially in the tropics and in East Asia remote from TCCON validation sites, we find larger spreads of about 1 ppm–2 ppm. This knowledge can be used to account for regional uncertainties in addition to the reported retrieval error estimates. Furthermore, it gives important indications where the most complicated retrieval conditions exist and where new validation sites would be of great interest.

TCCON is continuously expanding and improving and currently the de facto validation standard. However, many important regions are not covered, its accuracy (∼ 0.8 ppm) is not significantly better than the user requirements for regional biases, and TCCON cannot measure under cloudy conditions. Therefore, complementary validation concepts, e.g. based on NOAA's AirCore system (Karion et al., 2010) which is currently in development are of great interest especially for future satellite missions.

A unified validation exercise showed that EMMA performs well at TCCON sites. This was somewhat expected because most of the algorithms perform similarly well here. In terms of station-to-station biases, TCCON's accuracy does not allow to identify significant differences between the analyzed algorithms.

The strength of EMMA lies in the reduction of the spatial and temporal bias patterns which can be analyzed with the global gridded level 3 data: (i) EMMA's fraction of obvious outliers (in terms of unrealistically large gradients and unrealistically large deviation from CT2011) is lower than for any individual algorithm. (ii) It has the smallest STDD to CT2011 (considered as our current knowledge about atmospheric CO_2 concentrations) and TCCON. (iii) Its N/S gradients are in third best agreement with CT2011 and in best agreement with TCCON and have the lowest scatter in case of CT2011 and the third lowest scatter in case of TCCON. (iv) EMMA's seasonal amplitude is in best agreement with CT2011 and second best with TCCON and has the lowest scatter in both cases.

ACPD
12, 23195–23217, 2012

In summary, EMMA performs very well in terms of the analyzed statistical quantities. As long as no individual retrieval algorithm meets the demanding user requirements, we conclude that EMMA is a promising candidate for inverse modeling studies.

Our study also showed that all algorithms consistently observe a N/S gradient being about 0.3 ppm–0.9 ppm larger and a seasonal (peak-to-peak) amplitude being about 1.5 ppm–2.0 ppm larger than modeled by CT2011. Both effects were estimated to be slightly less pronounced in CT2010.

Future EMMA versions will profit from improvements of the individual algorithms. Furthermore, it is planned to extend the EMMA period to more years as soon as all algorithms have provided data.

Additional to EMMA v1.3a (described in this paper), we generated a version without WFMD (EMMA v1.3b) and a version without SCIAMACHY (EMMA v1.3c). EMMA seems to be very stable because rejecting, e.g. WFMD from the ensemble has only minor influence on the global maps and level 3 statistics. However, a relatively large influence can be observed in the patterns of the ensemble spread. Additionally, the single measurement precision (compare Table 2) is reduced to about 2 ppm for v1.3b and v1.3c. All EMMA versions are available upon request to download at http://www.iup.uni-bremen.de/~mreuter/emma.php.

Acknowledgements. This work was in part funded by ESA/ESRIN (GHG-CCI), EU FP7 (MACC-II), DLR (SADOS), and the State and the University of Bremen. We thank the members of the GOSAT Project (JAXA, NIES, and Ministry of the Environment Japan) for providing GOSAT Level 1B product (spectral data). The ACOS v2.9 data were produced by the ACOS/OCO-2 project at the Jet Propulsion Laboratory, California Institute of Technology, and obtained from the ACOS/OCO-2 data archive maintained at the NASA Goddard Earth Science Data and Information Services Center. We thank NOAA for making available the CarbonTracker CO_2 fields. We thank TCCON (and funding organizations; NASA grants NNX11AG01G, NAG5-12247, NNG05-GD07G, NASA Orbiting Carbon Observatory Program, DOE ARM program, the Australian Research Council, DP0879468 and LP0562346, the EU projects IMECC and GEOmon, the Senate of Bremen) and in particular N. Deutscher, D. Griffith, J. Notholt, R. Sussmann, P. Wennberg, D. Wunch for making available the XCO_2 data.

ACPD
12, 23195–23217, 2012

References

Araujo, M. B. and New, M.: Ensemble forecasting of species distributions, Trends Ecol. Evol., 22, 42–47, doi:10.1016/j.tree.2006.09.010, 2007. 23199

Bösch, H., Toon, G. C., Sen, B., Washenfelder, R. A., Wennberg, P. O., Buchwitz, M., de Beek, R., Burrows, J. P., Crisp, D., Christi, M., Connor, B. J., Natraj, V., and Yung, Y. L.: Space-based near-infrared CO_2 measurements: testing the orbiting carbon observatory retrieval algorithm and validation concept using SCIAMACHY observations over Park Falls, Wisconsin, J. Geophys. Res., 111, D23302, doi:10.1029/2006JD007080, 2006. 23198

Bösch, H., Baker, D., Connor, B., Crisp, D., and Miller, C.: Global Characterization of CO_2 Column Retrievals from Shortwave-Infrared Satellite Observations of the Orbiting Carbon Observatory-2 Mission, Remote Sens., 3, 270–304, doi:10.3390/rs3020270, 2011. 23198

Butz, A., Hasekamp, O. P., Frankenberg, C., and Aben, I.: Retrievals of atmospheric CO_2 from simulated space-borne measurements of backscattered near-infrared sunlight: accounting for aerosol effects, Appl. Opt., 48, 3322–3336, 2009. 23198

Butz, A., Guerlet, S., Hasekamp, O., Schepers, D., Galli, A., Aben, I., Frankenberg, C., Hartmann, J. M., Tran, H., Kuze, A., Keppel-Aleks, G., Toon, G., Wunch, D., Wennberg, P., Deutscher, N., Griffith, D., Macatangay, R., Messerschmidt, J., Notholt, J., and Warneke, T.: Toward accurate CO_2 and CH_4 observations from GOSAT, Geophys. Res. Lett., 38, L14812, doi:10.1029/2011GL047888, 2011. 23198

Chevallier, F., Bréon, F.-M., and Rayner, P. J.: Contribution of the orbiting carbon observatory to the estimation of CO_2 sources and sinks: theoretical study in a variational data assimilation framework, J. Geophys. Res., 112, D09307, doi:10.1029/2006JD007375, 2007. 23197, 23198

Crisp, D., Fisher, B. M., O'Dell, C., Frankenberg, C., Basilio, R., Bösch, H., Brown, L. R., Castano, R., Connor, B., Deutscher, N. M., Eldering, A., Griffith, D., Gunson, M., Kuze, A., Mandrake, L., McDuffie, J., Messerschmidt, J., Miller, C. E., Morino, I., Natraj, V., Notholt, J., O'Brien, D. M., Oyafuso, F., Polonsky, I., Robinson, J., Salawitch, R., Sherlock, V., Smyth, M., Suto, H., Taylor, T. E., Thompson, D. R., Wennberg, P. O., Wunch, D., and Yung, Y. L.: The ACOS CO_2 retrieval algorithm – Part II: Global X_{CO_2} data characterization, Atmos. Meas. Tech., 5, 687–707, doi:10.5194/amt-5-687-2012, 2012. 23197

ACPD
12, 23195–23217, 2012

Hagedorn, R., Doblas-Reyes, F., and Palmer, T.: The rationale behind the success of multi-model ensembles in seasonal forecasting – I. Basic concept, Tellus Ser. A, 57, 219–233, doi:10.1111/j.1600-0870.2005.00103.x, 2005. 23199

Heymann, J., Schneising, O., Reuter, M., Buchwitz, M., Rozanov, V. V., Velazco, V. A., Bovensmann, H., and Burrows, J. P.: SCIAMACHY WFM-DOAS XCO_2: comparison with CarbonTracker XCO_2 focusing on aerosols and thin clouds, Atmos. Meas. Tech., 5, 1935–1952, doi:10.5194/amt-5-1935-2012, 2012. 23198

Houweling, S., Breon, F.-M., Aben, I., Rödenbeck, C., Gloor, M., Heimann, M., and Ciais, P.: Inverse modeling of CO_2 sources and sinks using satellite data: a synthetic inter-comparison of measurement techniques and their performance as a function of space and time, Atmos. Chem. Phys., 4, 523–538, doi:10.5194/acp-4-523-2004, 2004. 23197

Karion, A., Sweeney, C., Tans, P., and Newberger, T.: AirCore: an innovative atmospheric sampling system, J. Atmos. Oceanic Technol., 27, 1839–1853, doi:10.1175/2010JTECHA1448.1, 2010. 23205

Keppel-Aleks, G., Wennberg, P. O., Washenfelder, R. A., Wunch, D., Schneider, T., Toon, G. C., Andres, R. J., Blavier, J.-F., Connor, B., Davis, K. J., Desai, A. R., Messerschmidt, J., Notholt, J., Roehl, C. M., Sherlock, V., Stephens, B. B., Vay, S. A., and Wofsy, S. C.: The imprint of surface fluxes and transport on variations in total column carbon dioxide, Biogeosciences, 9, 875–891, doi:10.5194/bg-9-875-2012, 2012. 23204

Kharin, V. and Zwiers, F.: Climate predictions with multimodel ensembles, J. Clim., 15, 793–799, doi:10.1175/1520-0442(2002)015<0793:CPWME>2.0.CO;2, 2002. 23199

Messerschmidt, J., Parazoo, N., Deutscher, N. M., Roehl, C., Warneke, T., Wennberg, P. O., and Wunch, D.: Evaluation of atmosphere-biosphere exchange estimations with TCCON measurements, Atmos. Chem. Phys. Discuss., 12, 12759–12800, doi:10.5194/acpd-12-12759-2012, 2012. 23204

Miller, C. E., Crisp, D., DeCola, P. L., Olsen, S. C., Randerson, J. T., Michalak, A. M., Alkhaled, A., Rayner, P., Jacob, D. J., Suntharalingam, P., Jones, D. B. A., Denning, A. S., Nicholls, M. E., Doney, S. C., Pawson, S., Bösch, H., Connor, B. J., Fung, I. Y., O'Brien, D., Salawitch, R. J., Sander, S. P., Sen, B., Tans, P., Toon, G. C., Wennberg, P. O., Wofsy, S. C., Yung, Y. L., and Law, R. M.: Precision requirements for space-based X_{CO_2} data, J. Geophys. Res., 112, D10314, doi:10.1029/2006JD007659, 2007. 23197, 23198

O'Dell, C. W., Connor, B., Bösch, H., O'Brien, D., Frankenberg, C., Castano, R., Christi, M., Eldering, D., Fisher, B., Gunson, M., McDuffie, J., Miller, C. E., Natraj, V., Oyafuso, F., Polon-

ACPD
12, 23195–23217, 2012

sky, I., Smyth, M., Taylor, T., Toon, G. C., Wennberg, P. O., and Wunch, D.: The ACOS CO_2 retrieval algorithm – Part 1: Description and validation against synthetic observations, Atmos. Meas. Tech., 5, 99–121, doi:10.5194/amt-5-99-2012, 2012. 23197

Oshchepkov, S., Bril, A., and Yokota, T.: PPDF-based method to account for atmospheric light scattering in observations of carbon dioxide from space, J. Geophys. Res.-Atmos., 113, D23210, doi:10.1029/2008JD010061, 2008. 23198

Oshchepkov, S., Bril, A., Maksyutov, S., and Yokota, T.: Detection of optical path in spectroscopic space-based observations of greenhouse gases: application to GOSAT data processing, J. Geophys. Res., 116, D14304, doi:10.1029/2010JD015352, 2011. 23198

Oshchepkov, S., Bril, A. T. Y., Morino, I., Yoshida, Y., Matsunaga, T., Belikov, D., Wunch, D., Wennberg, P., Toon, G., O'Dell, C., Butz, A., Guerlet, S., Cogan, A., Bösch, H., Eguchi, N., Deutscher, N., Griffith, D., Macatangay, R., Notholt, J., Sussmann, R., Rettinger, M., Sherlock, V., Robinson, J., Kyrö, E., Heikkinen, P., Feist, D., Nagahama, T., Kadygrov, N., Maksyutov, S., Uchino, O., and Watanabe, H.: Effects of atmospheric light scattering on spectroscopic observations of greenhouse gases from space. Part 1: validation of PPDF-based CO_2 retrievals from GOSAT, J. Geophys. Res., 117, D12305, doi:10.1029/2012JD017505, 2012. 23198

Peters, W., Jacobson, A. R., Sweeney, C., Andrews, A. E., Conway, T. J., Masarie, K., Miller, J. B., Bruhwiler, L. M. P., Pétron, G., Hirsch, A. I., Worthy, D. E. J., van der Werf, G. R., Randerson, J. T., Wennberg, P. O., Krol, M. C., and Tans, P. P.: An atmospheric perspective on North American carbon dioxide exchange: CarbonTracker, in: Proceedings of the National Academy of Sciences (PNAS) of the United States of America, November 27, 2007, 104, 18925–18930, 2007. 23198

Peters, W., Krol, M. C., van der Werf, G. R., Houweling, S., Jones, C. D., Hughes, J., Schaefer, K., Masarie, K. A., Jacobson, A. R., Miller, J. B., Cho, C. H., Ramonet, M., Schmidt, M., Ciattaglia, L., Apadula, F., Helta, D., Meinhardt, F., di Sarra, A. G., Piacentino, S., Sferlazzo, D., Aalto, T., Hatakka, J., Strom, J., Haszpra, L., Meijer, H. A. J., van der Laan, S., Neubert, R. E. M., Jordan, A., Rodo, X., Morgui, J. A., Vermeulen, A. T., Popa, E., Rozanski, K., Zimnoch, M., Manning, A. C., Leuenberger, M., Uglietti, C., Dolman, A. J., Ciais, P., Heimann, M., and Tans, P. P.: Seven years of recent European net terrestrial carbon dioxide exchange constrained by atmospheric observations, Global Change Biol., 16, 1317–1337, doi:10.1111/j.1365-2486.2009.02078.x, 2010. 23198

ACPD
12, 23195–23217, 2012

Rayner, P. J. and O'Brien, D. M.: The utility of remotely sensed CO_2 concentration data in surface inversions, Geophys. Res. Lett., 28, 175–178, 2001. 23197

Reuter, M., Buchwitz, M., Schneising, O., Heymann, J., Bovensmann, H., and Burrows, J. P.: A method for improved SCIAMACHY CO_2 retrieval in the presence of optically thin clouds, Atmos. Meas. Tech., 3, 209–232, doi:10.5194/amt-3-209-2010, 2010. 23197

Reuter, M., Bovensmann, H., Buchwitz, M., Burrows, J. P., Connor, B. J., Deutscher, N. M., Griffith, D. W. T., Heymann, J., Keppel-Aleks, G., Messerschmidt, J., Notholt, J., Petri, C., Robinson, J., Schneising, O., Sherlock, V., Velazco, V., Warneke, T., Wennberg, P. O., and Wunch, D.: Retrieval of atmospheric CO_2 with enhanced accuracy and precision from SCIAMACHY: validation with FTS measurements and comparison with model results., J. Geophys. Res., 116, D04301, doi:10.1029/2010JD015047, 2011. 23197, 23200, 23202, 23204

Reuter, M., Buchwitz, M., Schneising, O., Hase, F., Heymann, J., Guerlet, S., Cogan, A. J., Bovensmann, H., and Burrows, J. P.: A simple empirical model estimating atmospheric CO_2 background concentrations, Atmos. Meas. Tech., 5, 1349–1357, doi:10.5194/amt-5-1349-2012, 2012. 23199

Rodgers, C. D.: Inverse Methods for Atmospheric Sounding: Theory and Practice, World Scientific Publishing, Singapore, 2000. 23200

Rötter, R. P., Carter, T. R., Olesen, J. E., and Porter, J. R.: Crop-climate models need an overhaul, Nat. Clim. Change, 1, 175–177, 2011. 23199

Schneising, O., Buchwitz, M., Reuter, M., Heymann, J., Bovensmann, H., and Burrows, J. P.: Long-term analysis of carbon dioxide and methane column-averaged mole fractions retrieved from SCIAMACHY, Atmos. Chem. Phys., 11, 2863–2880, doi:10.5194/acp-11-2863-2011, 2011. 23198, 23204

Schneising, O., Bergamaschi, P., Bovensmann, H., Buchwitz, M., Burrows, J. P., Deutscher, N. M., Griffith, D. W. T., Heymann, J., Macatangay, R., Messerschmidt, J., Notholt, J., Rettinger, M., Reuter, M., Sussmann, R., Velazco, V. A., Warneke, T., Wennberg, P. O., and Wunch, D.: Atmospheric greenhouse gases retrieved from SCIAMACHY: comparison to ground-based FTS measurements and model results, Atmos. Chem. Phys., 12, 1527–1540, doi:10.5194/acp-12-1527-2012, 2012. 23198

Stephens, B. B., Gurney, K. R., Tans, P. P., Sweeney, C., Peters, W., Bruhwiler, L., Ciais, P., Ramonet, M., Bousquet, P., Nakazawa, T., Aoki, S., Machida, T., Inoue, G., Vinnichenko, N., Lloyd, J., Jordan, A., Heimann, M., Shibistova, O., Langenfelds, R. L., Steele, L. P., Francey, R. J., and Denning, A. S.: Weak northern and strong tropical

ACPD
12, 23195–23217, 2012

land carbon uptake from vertical profiles of atmospheric CO_2, Science, 316, 1732–1735, doi:10.1126/science.1137004, 2007. 23197

Tebaldi, C. and Knutti, R.: The use of the multi-model ensemble in probabilistic climate projections, Philos. Trans. R. Soc., A, 365, 2053–2075, doi:10.1098/rsta.2007.2076, 2007. 23199

Vautard, R., Schaap, M., Bergstrom, R., Bessagnet, B., Brandt, J., Builtjes, P. J. H., Christensen, J. H., Cuvelier, C., Foltescu, V., Graff, A., Kerschbaumer, A., Krol, M., Roberts, P., Rouil, L., Stern, R., Tarrason, L., Thunis, P., Vignati, E., and Wind, P.: Skill and uncertainty of a regional air quality model ensemble, Atmos. Environ., 43, 4822–4832, doi:10.1016/j.atmosenv.2008.09.083, 2009. 23199

Washenfelder, R. A., Toon, G. C., Blavier, J.-F., Yang, Z., Allen, N. T., Wennberg, P. O., Vay, S. A., Matross, D. M., and Daube, B. C.: Carbon dioxide column abundances at the Wisconsin Tall Tower site, J. Geophys. Res., 111, D22305, doi:10.1029/2006JD007154, 2006. 23198

Wunch, D., Toon, G. C., Wennberg, P. O., Wofsy, S. C., Stephens, B. B., Fischer, M. L., Uchino, O., Abshire, J. B., Bernath, P., Biraud, S. C., Blavier, J.-F. L., Boone, C., Bowman, K. P., Browell, E. V., Campos, T., Connor, B. J., Daube, B. C., Deutscher, N. M., Diao, M., Elkins, J. W., Gerbig, C., Gottlieb, E., Griffith, D. W. T., Hurst, D. F., Jiménez, R., Keppel-Aleks, G., Kort, E. A., Macatangay, R., Machida, T., Matsueda, H., Moore, F., Morino, I., Park, S., Robinson, J., Roehl, C. M., Sawa, Y., Sherlock, V., Sweeney, C., Tanaka, T., and Zondlo, M. A.: Calibration of the Total Carbon Column Observing Network using aircraft profile data, Atmos. Meas. Tech., 3, 1351–1362, doi:10.5194/amt-3-1351-2010, 2010. 23203

Wunch, D., Toon, G. C., Blavier, J.-F. L., Washenfelder, R. A., Notholt, J., Connor, B. J., Griffith, D. W. T., Sherlock, V., and Wennberg, P. O.: The Total Carbon Column Observing Network (TCCON), Phil. Trans. R. Soc. A, 369, 2087–2112, doi:10.1098/rsta.2010.0240, 2011. 23198, 23203

Yang, Z., Washenfelder, R. A., Keppel-Aleks, G., Krakauer, N. Y., Randerson, J. T., Tans, P. P., Sweeney, C., and Wennberg, P. O.: New constraints on Northern Hemisphere growing season net flux, Geophys. Res. Lett., 34, L12807, doi:10.1029/2007GL029742, 2007. 23204

Yoshida, Y., Ota, Y., Eguchi, N., Kikuchi, N., Nobuta, K., Tran, H., Morino, I., and Yokota, T.: Retrieval algorithm for CO_2 and CH_4 column abundances from short-wavelength infrared spectral observations by the Greenhouse gases observing satellite, Atmos. Meas. Tech., 4, 717–734, doi:10.5194/amt-4-717-2011, 2011.

23197

ACPD

12, 23195–23217, 2012

Table 1. Main retrieval characteristics: algorithm name and version, satellite instrument, spectral bands, inversion technique (OE = optimal estimation, TP = Tikhonov – Phillips regularization, LS = least squares), consideration of scattering (FP = full physics, PR = light path proxy, PPDF = photon path length probability density function, 4EP20 = 4 extinction profiles with 20 layers (two aerosol types, water and ice cloud), CWP = cloud water path, CTH = cloud top height, APSx = aerosol profile scaling of x different aerosol types, AOD = aerosol optical depth, SLR = reflectivity of scattering layer, PLMP = path length modification parameter, APNC = aerosol particle number concentration, ASP = aerosol size parameter, AH = aerosol height, CEPS = cloud extinction profile scaling), main cloud filter (CAI = cloud and aerosol imager of GOSAT, PMD = polarization measurement device of SCIAMACHY).

Algorithm	Sensor	Bands (μm)				Inversion	CO_2 a Priori	Scattering	Main Cloud Filter	Empirical Bias Correction
		0.76	1.58	1.60	2.05					
ACOS v2.9	GOSAT	•		•	•	OE	model	FP (4EP20)	O_2-A	•
BESD v01.00.01	SCIAMACHY	•	•			OE	static	FP (CWP, CTH, APS1)	MERIS	•
NIES v02.xx	GOSAT	•		•	•	OE	model	FP (AOD)	CAI	
PPDF-DOAS	GOSAT	•		•	•	OE	static	PPDF (RSL, PLMP)	CAI	
RemoteC v1.0	GOSAT	•		•	•	PT	static	FP (APNC, ASP, AH)	CAI	•
UOL-FP v3.0	GOSAT	•		•	•	OE	model	FP (APS2, CEPS)	O_2-A	•
WFMD v2.2bcv7b	SCIAMACHY	•	•			LS	static	PR (CO_2/O_2)	PMD	•

ACPD
12, 23195–23217, 2012

Table 2. Validation statistics (June 2009–May 2010) for all TCCON sites with more than ten co-locations (Białystok, Poland; Darwin, Australia; Garmisch-Partenkirchen, Germany; Lamont, USA; Orléans, France; Park Falls, USA; Wollongong, Australia) with number of co-locations (#), average single measurement precision (σ), and standard deviation of station-to-station biases (Δ).

Algorithm	#	σ (ppm)	Δ (ppm)
ACOS v2.9	1530	2.1	0.9
BESD v01.00.01	2789	2.3	0.9
NIES PPDF-D	460	3.1	0.8
NIES v02.xx	1062	1.9	0.7
RemoteC v1.0	1084	2.5	0.9
UOL-FP v3.0	1086	2.3	0.8
WFMD v2.2bcv7b	8884	4.4	1.3
EMMA v1.3a	**1595**	**3.1**	**0.8**

ACPD
12, 23195–23217, 2012

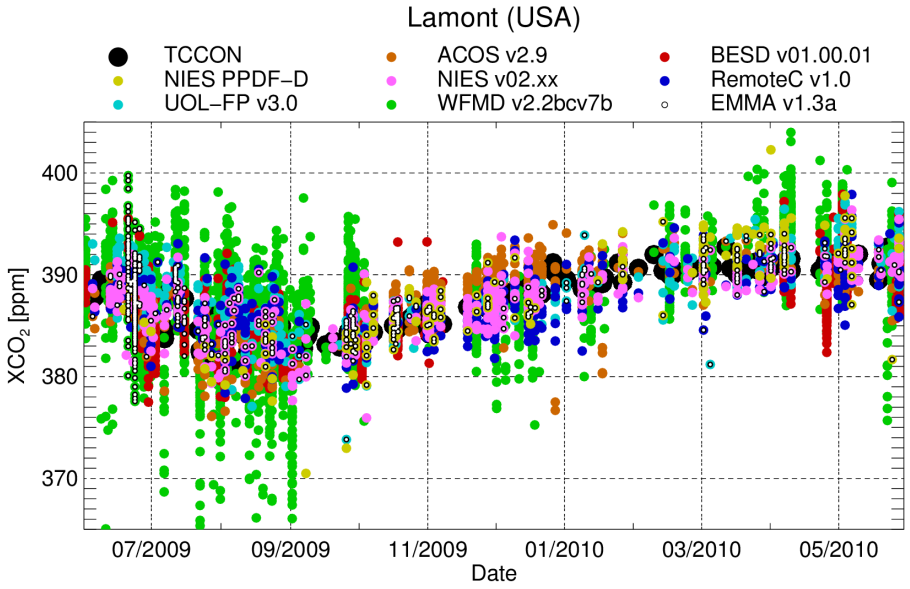

Fig. 1. Co-locations with validation measurements at the TCCON site Lamont, USA (distance < 500 km, time difference < 2 h). Highlighted are soundings included in EMMA.

ACPD
12, 23195–23217, 2012

The ensemble median algorithm EMMA

M. Reuter et al.

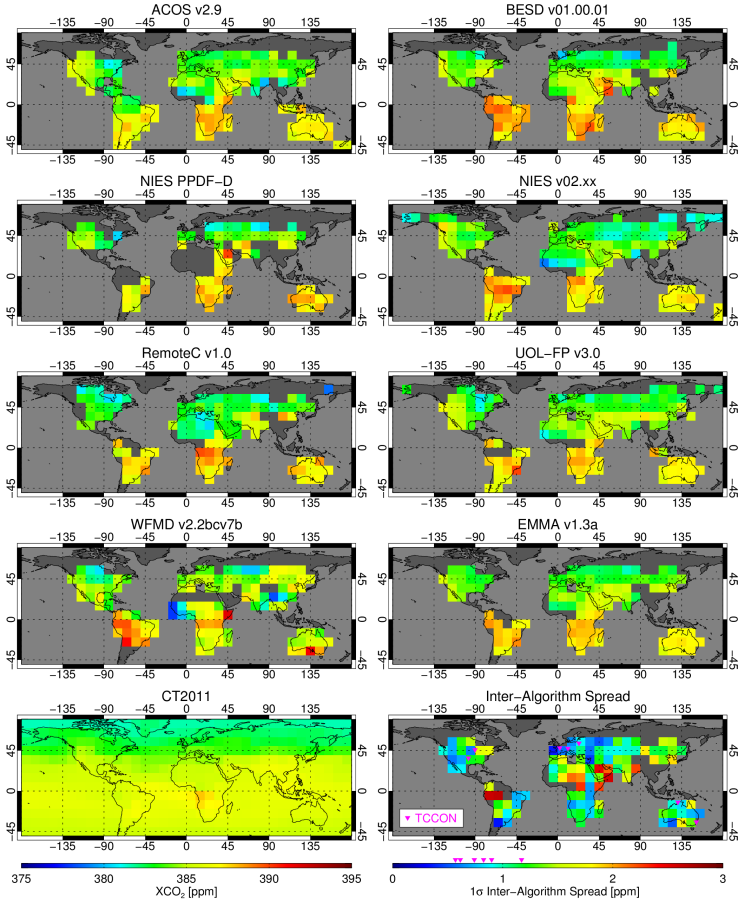

Fig. 2. Typical monthly gridded averages (September 2009) of the seven algorithms, EMMA, and CT2011 as well as corresponding inter-algorithm spread, i.e. the inter-algorithm standard deviation.

ACPD
12, 23195–23217, 2012

The ensemble median algorithm EMMA

M. Reuter et al.

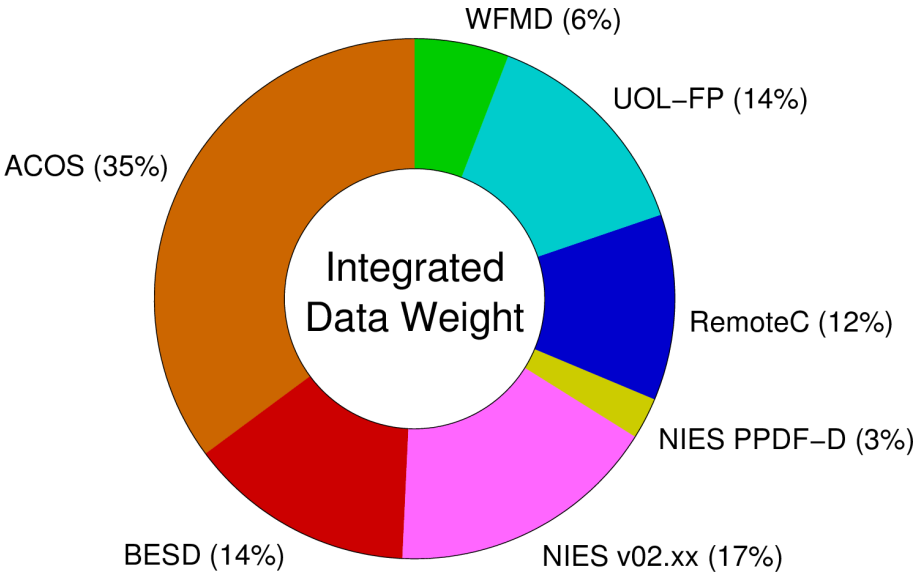

Fig. 3. Integrated data weight of each algorithm within the EMMA database defined as $\sum 1/\sigma_i^2$ where σ_i is the (scaled) individual sounding error.

ACPD
12, 23195–23217, 2012

The ensemble median algorithm EMMA

M. Reuter et al.

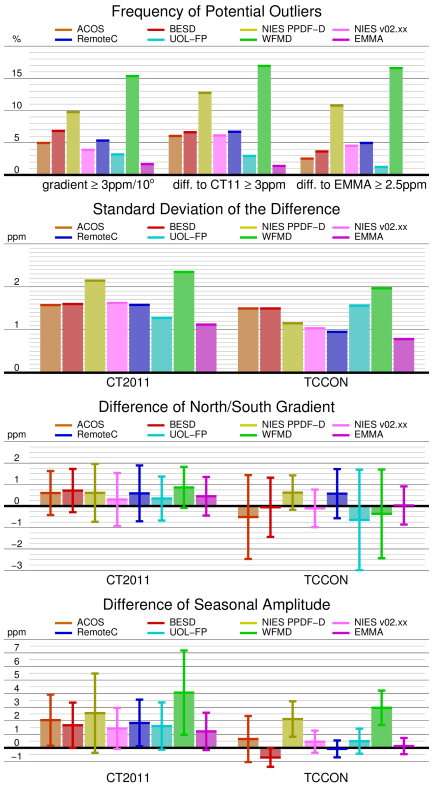

Fig. 4. Performance statistics (based on level 3 data) of the seven individual retrieval algorithms and EMMA. From top to bottom: frequency of potential outliers defined as unrealistically large spatial gradient, large deviation from CT2011, and large deviation from EMMA; standard deviation of the difference (STDD) to CT2011 and TCCON; difference of the north/south gradient to CT2011 and TCCON (average and standard deviation); difference of the seasonal amplitude to CT2011 and TCCON (average and standard deviation).

ACPD
12, 23195–23217, 2012